Heliyon 10 (2024) e25570

Contents lists available at ScienceDirect

Heliyon

journal homepage: www.cell.com/heliyon

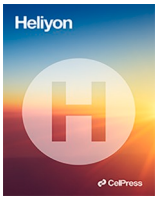

Research article

A robust primary liver cancer subtype related to prognosis and drug response based on a multiple combined classifying strategy

Jielian Deng [a,d], Guichuan Lai [a], Cong Zhang [a], Kangjie Li [a], Wenyan Zhu [b,c,d,**], Biao Xie [a,***], Xiaoni Zhong [a,*]

[a] Department of Epidemiology and Health Statistics, School of Public Health, Chongqing Medical University, Chongqing, China
[b] Chongqing Engineering Research Center of Pharmaceutical Sciences, Chongqing Medical and Pharmaceutical College, Chongqing, China
[c] College of Pharmacy, Chongqing Medical University, Chongqing, China
[d] Medical Department, Yidu Cloud (Beijing) Technology Co., Beijing, China

ARTICLE INFO

Keywords:
Prognostic markers
Cancer molecular markers
Cancer stem cells
Immune microenvironment
Genotyping
Combined classifying
Drug sensitivity

ABSTRACT

The recurrence or resistance to treatment of primary liver cancer (PLL) is significantly related to the heterogeneity present within the tumor. In this study, we integrated prognosis risk score, mRNAsi index, and immune characteristics clustering to classify patients. The four subtypes obtained from the combined classification are associated with PLC's prognosis and drug response. In these subtypes, we observed mRNAsiH_ICCA subtype, the intersection between high mRNAsi and immune characteristics clustering A, had the worst prognosis. Specifically, immune characteristics clustering B (ICC_B) had high drug sensitivity in most drugs regardless of the value of mRNAsi. On the other hand, patients with low mRNAsi responded better to ten drugs including KU-55933 and NU7441, while patients with high mRNAsi might benefit from drugs like Leflunomide. By matching the specific characteristics of each combined subtype with the drug-induced cell line expression profile, we identified a group of potential therapeutic drugs that might regulate the expression of disease signature genes. We developed a feasible multiple combined typing strategy, hoping to guide therapeutic selection and promote the development of precision medicine.

1. Introduction

Primary liver cancer (PLC) is a common cause of cancer-related morbidity and death [1]. In 2020, there were about 906,000 new PLC cases and 830,000 deaths worldwide, accounting for the third place in global cancer deaths [2,3]. Now clinical research has proven that surgical resection, transplantation, ablation, transarterial chemoembolization, immune checkpoint inhibitors, and the tyrosine-kinase inhibitors sorafenib are treatments with survival benefits [4–6]. However, specific drugs or treatments can only be beneficial in some patients, and the risk of recurrence or drug resistance still exists [4]. Therefore, more researches are needed for the guidance of PLC therapeutic selection.

* Corresponding author.
** Corresponding author. Chongqing Engineering Research Center of Pharmaceutical Sciences, Chongqing Medical and Pharmaceutical College, Chongqing, China.
*** Corresponding author.
E-mail addresses: zhuwy_julie@163.com (W. Zhu), kybiao@cqmu.edu.cn (B. Xie), zhongxiaoni@cqmu.edu.cn (X. Zhong).

https://doi.org/10.1016/j.heliyon.2024.e25570
Received 16 April 2023; Received in revised form 13 January 2024; Accepted 29 January 2024
Available online 1 February 2024

Tumor heterogeneity is caused by changes in molecular biology or genes during tumor growth and makes differences in tumor growth rate, invasion ability, drug sensitivity, prognosis, etc. [7–9]. Solid tumors are composed of different cell collections and are complex networks including tumor cells, infiltrating immune cells, endothelial cells, stromal cells, and extracellular matrix [10]. The interaction between tumor cells and their surrounding microenvironment promotes the heterogeneity between tumors [11,12]. Evidence is mounting that cancer stem cells (CSCs) are one of the determinants of intratumoral heterogeneity [13]. CSCs can regenerate all the characteristics of tumors because of their specific stem cell-like self-renewal and differentiation abilities, which are the roots of tumor recurrence and drug resistance [14]. The heterogeneity of tumor immune microenvironment(TIME) is an important source of tumor heterogeneity [15,16]. Patients resist the malignant proliferation of tumor cells through their unique immune response, but the reprogrammed immune response might promote tumor immune escape, metastasis and recurrence [17].

Tumor heterogeneity was the basis of patients' prognoses and treatment response differences. Based on tumor heterogeneity, classifying subtypes through biomarkers and carrying out precise treatment was meaningful. Previous studies have classified PLC from different perspectives. Multiple prognosis prediction models built by machine learning algorithms, including random forest and LASSO regression, were utilized as prognostic risk stratification tools. For example, three genes from microvascular invasion were utilized to evaluate the overall survival of liver cancer, and the prediction accuracy could reach 0.740 (1 year), 0.664 (2 years), and 0.693 (3 years) [18]. The index accuracy of the new m1A scoring model related to the immune microenvironment reached 0.71, 0.69, and 0.74 [19]. Considering the important influence of tumor stem cells on tumor growth, Wang et al. adopted one-class Logistic regression (OCLR) algorithm to quantify the ability of tumor dedifferentiation, dividing patients into subgroups representing different prognoses and drug resistance [20]. Using the immune characteristics of TIME to classify tumor samples, Hu found that the subtypes with better immune features usually responded well to immunotherapy [21].

The occurrence and development of tumor was a complex mechanism, tumor cell heterogeneity and immunosuppressive TIME were independent but cooperative driving factors of tumor progression, and also the basis of drug resistance [22]. However, many existing researches employed single stratification strategies which cannot distinguish PLC patients well. This study aims to develop a novel combined classifying strategy based on these common stratification methods, dividing patients with different prognoses and drug responses more precisely. Moreover, the treatment response and targeted strategies of these heterogeneous subtypes in those studies had not been further explored. We will infer the drug sensitivity of combined subtypes and identify potential small molecular compound drugs, further expanding the treatment options of patients with PLC.

2. Materials and methods

2.1. Data collection and processing

We downloaded the transcriptome, clinical, and follow-up data of The Cancer Genome Atlas Liver Hepatocellular Carcinoma project (TCGA-LIHC) from UCSC Xena (https://xenabrowser.net/) [23]. Additionally, we obtained similar data of the River Cancer - RIKEN, JP (ICGC-LIRI) cohort from the International Cancer Genome Consortium database (https://dcc.icgc.org/). These databases have already conducted comprehensive preprocessing on the uploaded data, and further details about these processing steps can be found on the database's website. After transcriptome and clinical information were matched, 363 PLC samples from the TCGA-LIHC cohort were included in our study as the training dataset. 50 normal samples were utilized as controls for disease gene identification, and the LIRI-JP cohort including 231 PLC patients was applied as an independent verification set. Except for the COUNT form used in the differential analysis, all the transcriptome data used in the other analysis were transformed to Transcripts Per Kilobase Million (TPM), and all the expression data were log2 transformed.

2.2. Prognostic gene screening and risk model construction

This study combined various methods for the risk model-building process. Firstly, we focused on those genes with large variations, which presented a median absolute deviation (MAD) value greater than 1 [24]. Secondly, the univariate Cox analysis was utilized to identify the genes related to prognosis, of which genes with a P value less than 0.05 were included for further analysis [25]. Thirdly, we randomly opted for 80 % patients to do univariate Cox analysis and repeated this operation 1000 times. The genes, with a P value less than 0.05 emerging more than 900 times, were considered stable and further analyzed [26]. Fourthly, we ran the random forest and LASSO to reduce the collinearity and further screened the genes. Finally, through the stepwise Cox regression method, we built the final model to evaluate the prognosis risk of patients.

2.3. Evaluation of stemness characteristics

OCLR is a binary classification algorithm and uses a logistic regression model to train a dataset containing only one class of samples. The trained model is then applied to new, unknown samples, and their probability values are used to determine whether they belong to the positive or negative class [27]. In this study, OCLR was employed to analyze and model the transcriptome data of stem cells. The mRNA stemness index (mRNAsi) in tumor samples was calculated to assess the stem cell similarity of the tumor samples [27,28]. We collected the gene expression profile of 93 stem cell samples from Progenitor Cell Biology Consortium (PCBC) data base (https://www.synapse.org/)and calculated the mRNAsi by the OCLR algorithm after the mRNA expression mean centering. Then the linear transformation was utilized to map the stemness index in the range of 0–1.

2.4. Immune characteristic clustering

We collected 29 immune-related gene sets (some details can be seen in Table S2) representing immune cells, pathways, and functions from the literature [29], and utilized the ssGSEA method to quantify the relevant characteristic scores by the R package "GSVA" [30]. Then, based on the k-means method of the R package "ConsensusClusterPlus" [31], the samples were clustered into different subtypes according to the immune characteristics by 1000 repeated consistency clustering. In order to fully evaluate the characteristics of immune subtypes, "CIBERSORT" was utilized to depict the infiltration of 28 kinds of immune cells [32], and "ESTIMATE" appraised the stromal cells and immune cells in tissues [33].

2.5. Functional enrichment analysis and somatic mutation analysis

We conducted GSEA enrichment analysis on the subgroups identified by the median of mRNAsi to reveal the differences in biological function. We utilized "clusterProfiler" package [34] and logged on the Gene Set Enrichment Analysis(GSEA,https://www.gsea-msigdb.org) to collect GO, KEGG pathways, and 50 marker gene sets. The gene expression differences between subgroups were analyzed through the "limma" package [35]. We employed "clusterProfiler" package to perform the GSEA enrichment of each gene set and selected the gene set with $p < 0.05$. Normalized enrichment scores (NES) evaluated the enrichment degree of subgroups on each gene set. In addition, the R package "Maftools" [36] was utilized to implement somatic mutation analysis to obtain the TMB of each liver cancer patient, and visualized the waterfall diagram in the high and low mRNAsi groups.

2.6. Drug efficacy inference of different subtypes

We use immune therapy prediction algorithms to evaluate the potential efficacy of immune therapy in patients with different expression profiles. The T-cell inflammation gene expression profile (GEP) score is calculated by evaluating 18 genes, which are related to antigen presentation, chemokine expression, cytotoxic activity, and adaptive immune resistance-associated IFN-γ response genes. The GEP score serves as a biomarker for inflammation in the tumor microenvironment (TME), and a higher GEP score indicates a higher probability of response to PD-1 blockade therapy [37,38]. The immune reactivity score (IMPRES) is calculated by analyzing the transcriptional relationships between 15 immune checkpoint genes [39], ranging from 0 to 15, with higher values indicating a higher probability of objective relief after immune checkpoint inhibitor therapy. Besides, the R package "oncoPredict" [40] was utilized to predict the response of small molecular drugs to the treatment of liver cancer samples. According to the semi-maximum inhibitory concentration (IC50) data of the medium cell line samples from Genomics of Drug Sensitivity in Cancer (GDSC, https://www.cancerrxgene.org), we integrated the expression profiles of the cell line and the PLC samples. The expression profiles were utilized to estimate the sensitivity of PLC patients to small and medium-sized molecular compounds in the database by ridge regression analysis, especially the first-line drug sorafenib and some drugs that had been reported to have potential therapeutic significance for PLC.

2.7. Potential drugs identification of different subtypes

The R package "limma" was utilized to screen the significantly different genes between each subgroup and normal samples, the genes were considered as reference disease genes for drug screening. Connectivity map (CMap) database (https://clue.io/) containing drug genome data could explore potential therapeutic compounds targeting disease genes according to the expression characteristics, and also reveal the mechanisms of action (MOA) of compounds targeting corresponding molecular pathways [41]. The top differentially expressed genes (DEGs) of each subtype compared with the normal sample was queried in the CMap database and the compounds with negative enrichment scores and $P < 0.05$ were considered potential therapeutic drugs for each subtype.

2.8. Statistical analysis

t-test was utilized for continuous data and the Chi-square test was utilized for classified data. The rank sum test was utilized to compare the classification variables and non-normal distribution variables of the two groups. The Pearson correlation test was utilized for the correlation between normal distribution variables, and the Spearman correlation test was utilized for the correlation between non-normal distribution variables. R software (4.1.1 version) was utilized for statistical analysis in this study. P value < 0.05 was considered statistically significant, and the odds ratio (ORs), hazard ratio (HRs), and 95 % confidence interval (CIs) were reported when necessary.

3. Results

3.1. Prognostic risk stratification of PLC based on gene characteristics

2232 genes with large variation were selected. Univariate Cox analysis identified 362 genes significantly related to prognosis among 2232 genes. Random forest was utilized to further obtain 311 genes. Through LASSO regression, a total of 31 genes were included in the multivariate Cox analysis (Fig. 1A). The final model included 12 genes and we calculated the sum of the genes' expression level and their corresponding coefficients of multivariate COX regression as the risk score of per patient. Risk Score =

(0.2682141 ∗ HOXD9 − 0.1979062 ∗ SLC16A11 − 0.1757526 ∗ PON1 − 0.2066533 ∗ NLRP6 − 0.4446951 ∗ KLRB1 - +0.1837433 ∗ AFF3 +0.2588551 ∗ S100A9 +0.3488320 ∗ SGCB − 0.3328202 ∗ SOCS2 +0.2188173 ∗ AGPAT5 +0.1771504 ∗ NINJ2 - +0.1309100 ∗ ALPK3). Among them, SLC16A11, PON1, NLRP6, KLRB1, and SOCS2 expressed lowly in the high-risk group and played a protective role while the other seven genes were highly expressed in the high-risk group and were dangerous factors (Fig. 1B).

The time-ROC curve displayed that the prediction model of 12 genes had good prognostic prediction ability. The AUC of 1, 2, 3, 4, and 5 years in the TCGA-LIHC data set was 0.845, 0.813, 0.813, 0.812, and 0.796, with the average AUC value of 1–5 years being higher than 0.8 (Fig. 1C and D). The AUC values of the LIRI-JP dataset in the 1, 2, and 3 years were 0.764, 0.663, and 0.691, respectively, indicating that the prediction model constructed by 12 genes also had fine prediction power in the independent

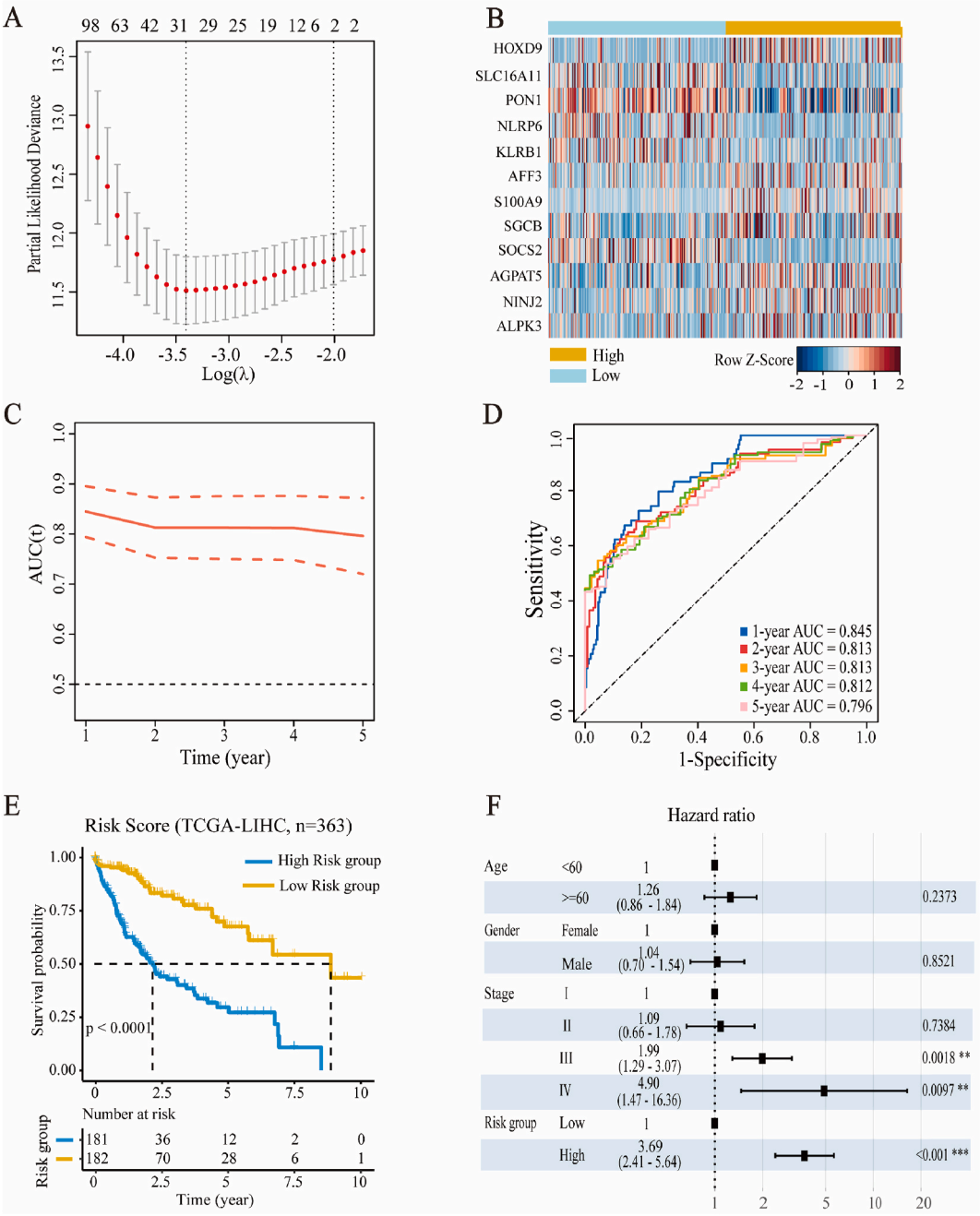

Fig. 1. Construction and evaluation of prognostic risk prediction model for PLC patients. (A) Result of LASSO regression analysis. (B)The heat map of 12 gene expression levels in prognostic risk model. (C) AUC value of prognostic risk model. (D) Time-dependent ROC curves for 1, 3 and 5 years. (E) Kaplan-Meier survival analysis and Log-rank test of patient's OS between high and low risk groups. (F) Forest plot of multivariate Cox regression analysis.

verification set (Figs. S1C and D). Compared with the performance of the previous relevant study's prognostic models (model A 0.8 [1 year], 0.69 [2 years], and 0.668 [3 years], model B 0.799 [1 year], 0.799 [2 years] and 0.801 [3 years]) [42,43], our model performed better than the existing models. Therefore, the prognostic model constructed in our study was able to predict the prognosis of patients better and could be extrapolated to other datasets for use, even characterizing the patients' survival risks in subsequent studies. In order to further evaluate the characteristics of the model, we divided the sample into high-risk and low-risk groups based on the median value of the risk score and carried out a Kaplan-Meier (KM) analysis. The results suggested that the risk score could distinguish two subgroups with different survival states in both the training set and the validation set, indicating that the 12-gene model could be used for risk stratification of liver cancer patients (Fig. 1E and Fig. S1E). In the two datasets, the 12-gene characteristic score was still an independent prognostic factor after adjusting for age, sex, and tumor stage (Fig. 1F and Fig. S1F).

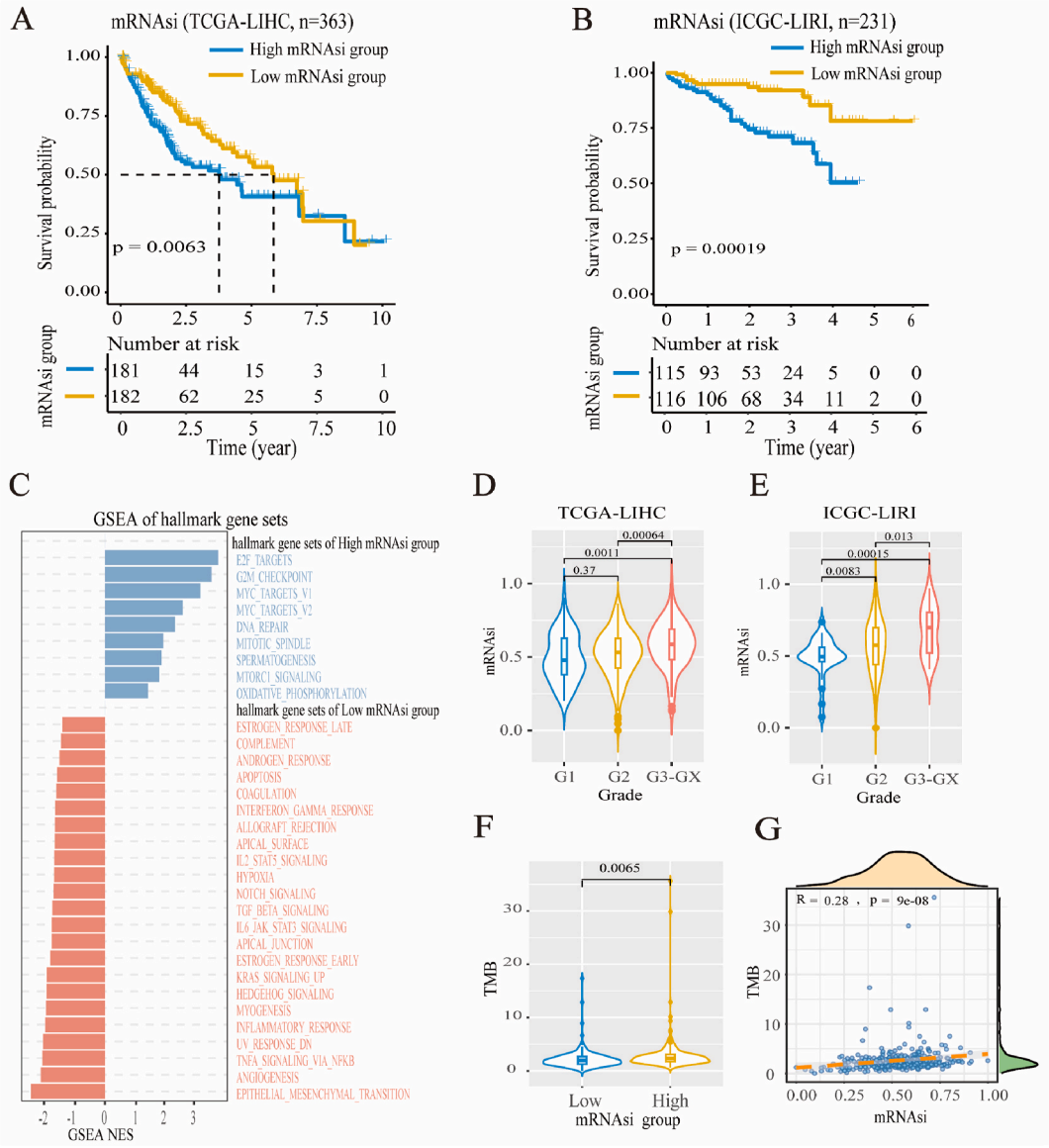

Fig. 2. Characteristics of PLC patients with high and low mRNAsi. (A) Kaplan-Meier survival analysis and Log-rank test of patient's OS between high and low mRNAsi groups in TCGA-LIHC cohort. (B) Kaplan-Meier survival analysis and Log-rank test of patient's OS between high and low mRNAsi groups in ICGC-LIRIcohort. (C) Marker gene set enrichment of differential expression genes (DEGs) between high and low mRNAsi groups. (D–E) mRNAsi distribution and comparison of different grades in TCGA-LIHC and ICGC-LIRI cohorts. (F) TMB distribution and comparison between high and low mRNAsi groups. (G) Correlation between mRNAsi and TMB.

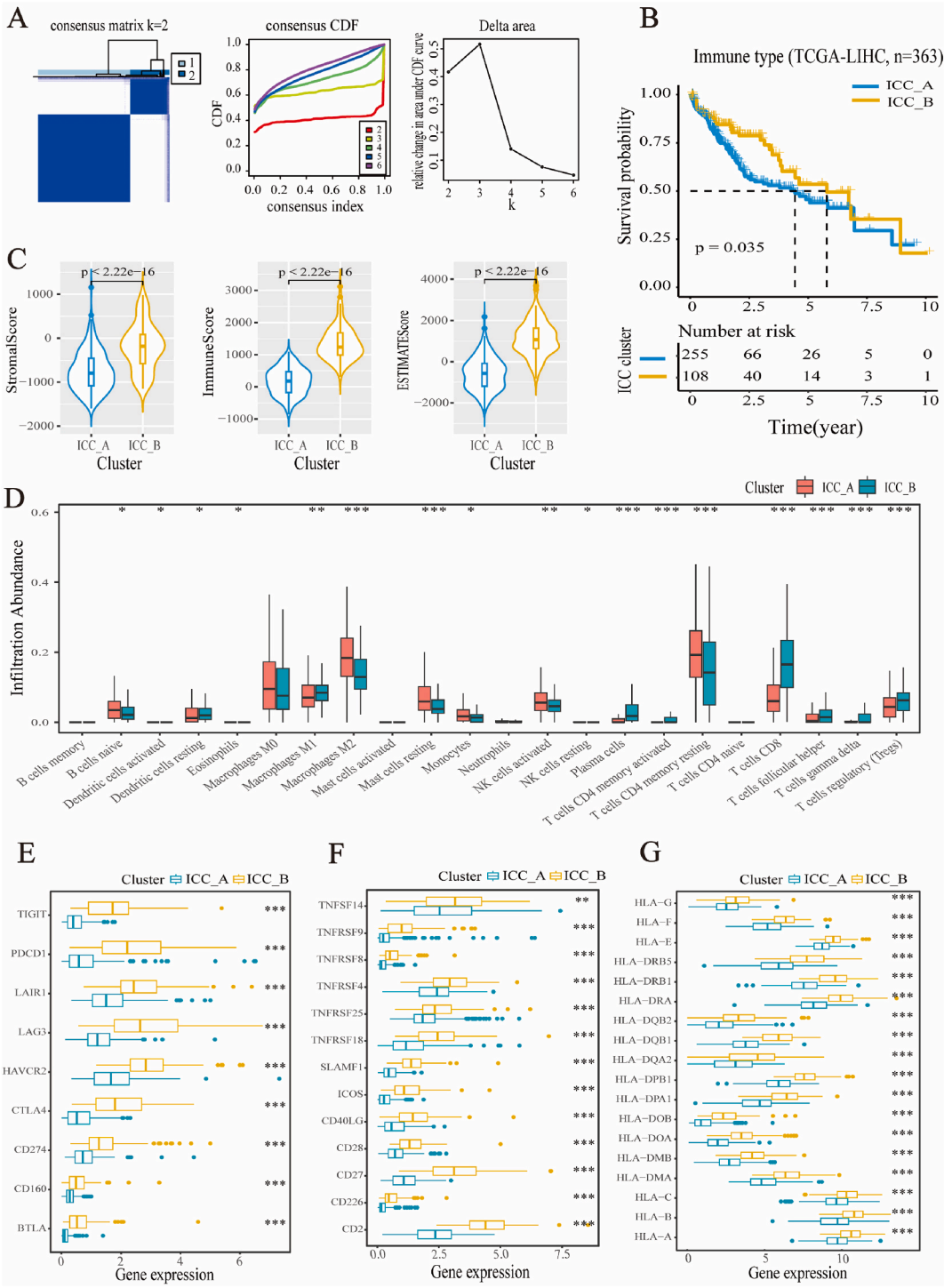

Fig. 3. The characteristics of immune subtypes in PLC patients. (A) Consensus matrix heatmap for two subtypes (k = 2). When k = 2–6, the correlation between CDF and consensus index under the consensus CDF curve. When k = 2–6, the relative change in area under the CDF curve. (B) Kaplan-Meier survival analysis and Log-rank test of patient's OS in the immune subtypes. (C) Distribution and comparison of StromalScore, ImmuneScore, and ESTIMATEScores in the immune subtypes. (D) Abundance of tumor-infiltrating immune cells in the immune subtypes. (E) Distribution and comparison of immune suppressive genes expression in the immune subtypes. (F) Distribution and comparison of immune activating genes expression in the immune subtypes. (G) Distribution and comparison of human leukocyte antigen genes expression in the immune subtypes.

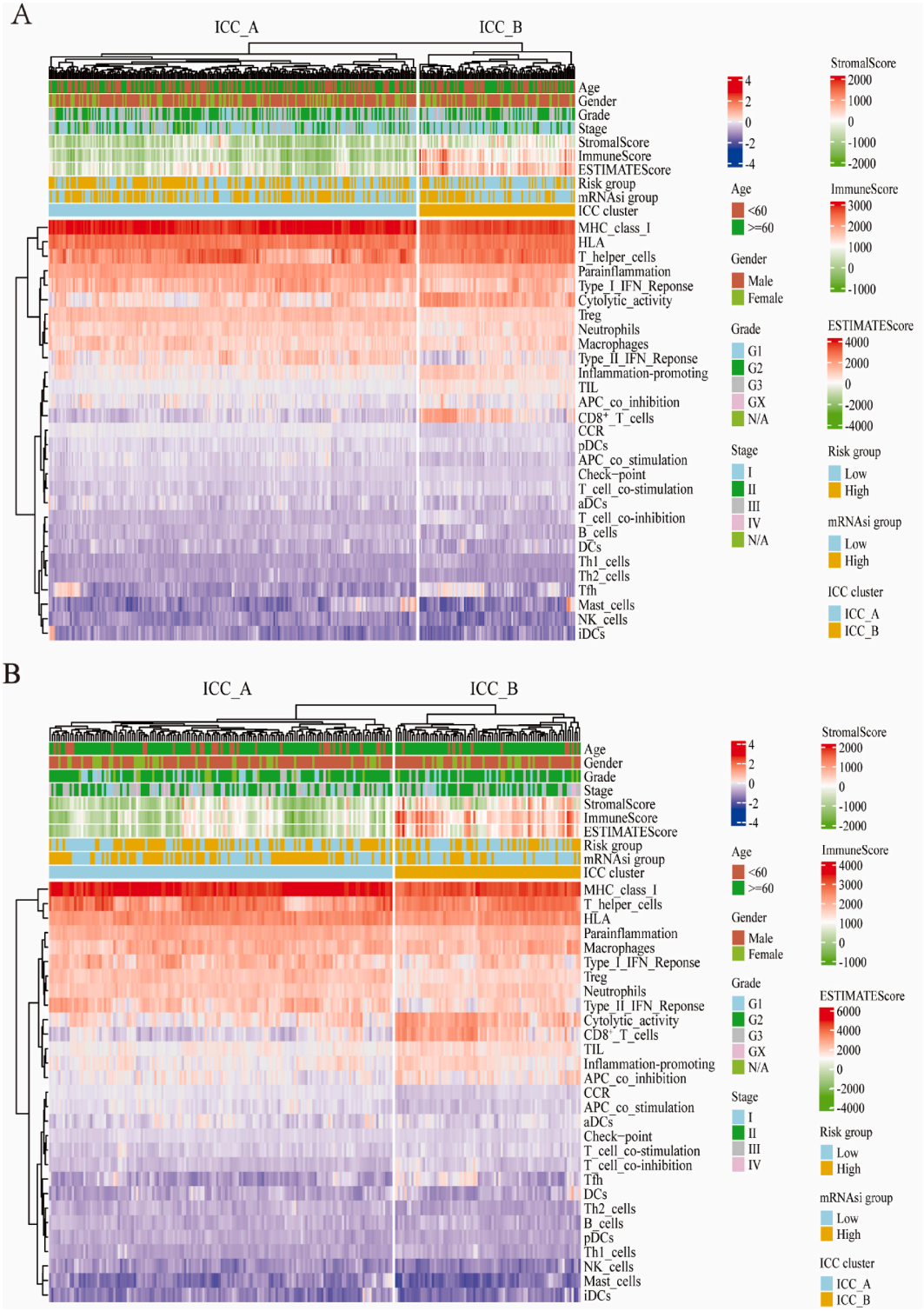

Fig. 4. Comprehensive heat map of subtypes, immune characteristics and clinical features of PLC patients. (A)The comprehensive heat map in TCGA-LIHC cohort. (B) The comprehensive heat map in ICGC-LIRI cohort.

3.2. mRNAsi index reveals heterogeneity in PLC

Based on the gene expression profile of 363 PLC patients, the mRNAsi was calculated by OCLR algorithm. There was a significant correlation between mRNAsi and histological grade in patients with liver cancer while no significant differences in mRNAsi were observed between the age subgroups, gender subgroups, and different diagnosis stages (Figs. S2C and D). In the TCGA-LIHC and ICGC-LIRI datasets, Fig. 2D and E indicate that higher histological grades correspond to higher dryness indices (except for G1 and G2).

363 GPL patients were divided into high mRNAsi and low mRNAsi groups based on the median of mRNAsi. KM survival analysis showed that the overall survival (OS) of the high mRNAsi group was better than that of the low mRNAsi group ($p = 0.0063$). In the ICGC-LIRI dataset, the survival advantage of the low mRNAsi group was also observed ($p = 0.00019$) (Fig. 2A and B). Considering the prognostic difference between the high mRNAsi and low mRNAsi groups, we further analyzed the functional enrichment of the high and low mRNAsi subgroups. Among the 50 marker genes, 9 marker genes were significantly enriched in the high mRNAsi group including E2F_ TARGETS, G2M_ CHECKPOINT, and MYC_ TARGETS_ V1/V2 while another 23 marker genes were concentrated in the low mRNAsi group. The GO enrichment analysis represented that large ribosomal subunit, cytosolic ribosome, negative regulation of chromosome segregation, and structural constituent of ribosome were significantly enriched in the high mRNAsi group whereas collagen trimer, collagen fibril organization, and extracellular matrix structural constituent were enriched in the other group. In the high mRNAsi group, 22 KEGG pathways including DNA replication, cell cycle, and oxidative phosphorylation, were significantly up-regulated, and other 112 KEGG pathways, including cell adhesion molecules, protein differentiation, and absorption, were significantly down-regulated (Fig. 2C and Figs. S2A and D).

Considering the characteristics of tumor stem cells may be derived from gene mutations, we analyzed the somatic mutations of GPL samples and observed a higher TMB ($p = 1.6e-05$) in the high mRNAsi group (Fig. 2F). TMB was significantly positively correlated with mRNAsi ($r = 0.28$, $p = 9e-08$) (Fig. 2G). In addition, the waterfall diagram of the two subgroups further interpreted the mutation

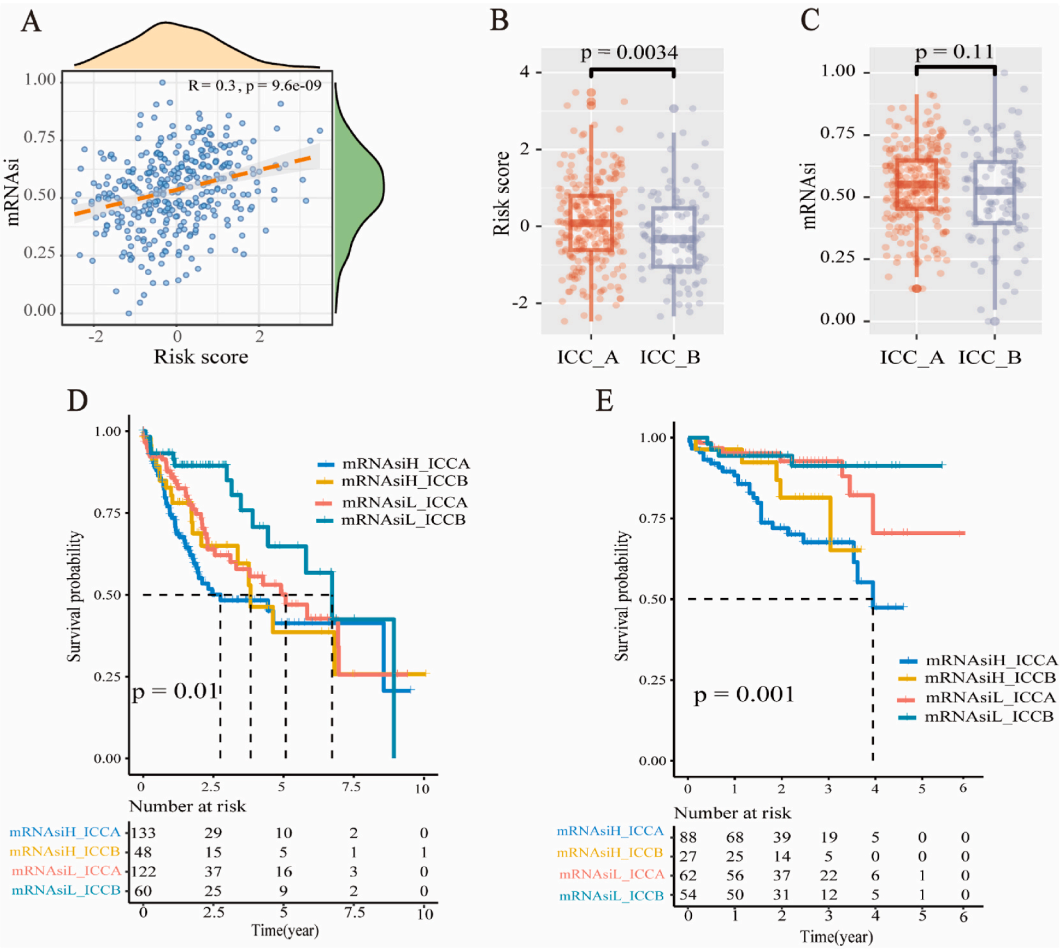

Fig. 5. Correlation of the three stratification methods and the survival significance of mixed subtypes. (A) Correlation of risk scores with mRNAsi. (B) Risk score distribution and comparison between immune subtypes. (C) mRNAsi distribution and comparison between immune isotypes. (D) Kaplan-Meier survival analysis and Log-rank test of patient's OS with mixed subtypes in the TCGA-LIHC cohort. (E) Kaplan-Meier survival analysis and Log-rank test of patient's OS with mixed subtypes in the ICGC-LIRI cohort.

landscape, which the mutation frequency of the high mRNAsi group is higher. The top 10 genes in the high mRNAsi group can be observed in most samples (86.29 %, 151/175), while the index was 69.49 %, 123/177 in the low mRNAsi. The titin (TTN) with the highest mutation frequency in all samples, was 37 % in the high mRNAsi group and 28 % in the low mRNAsi group. Notably, 31 % of the TP53 mutations were in second place in the high mRNAsi group but only 14 % in the low mRNAsi group were in fifth place (Figs. S2E and F).

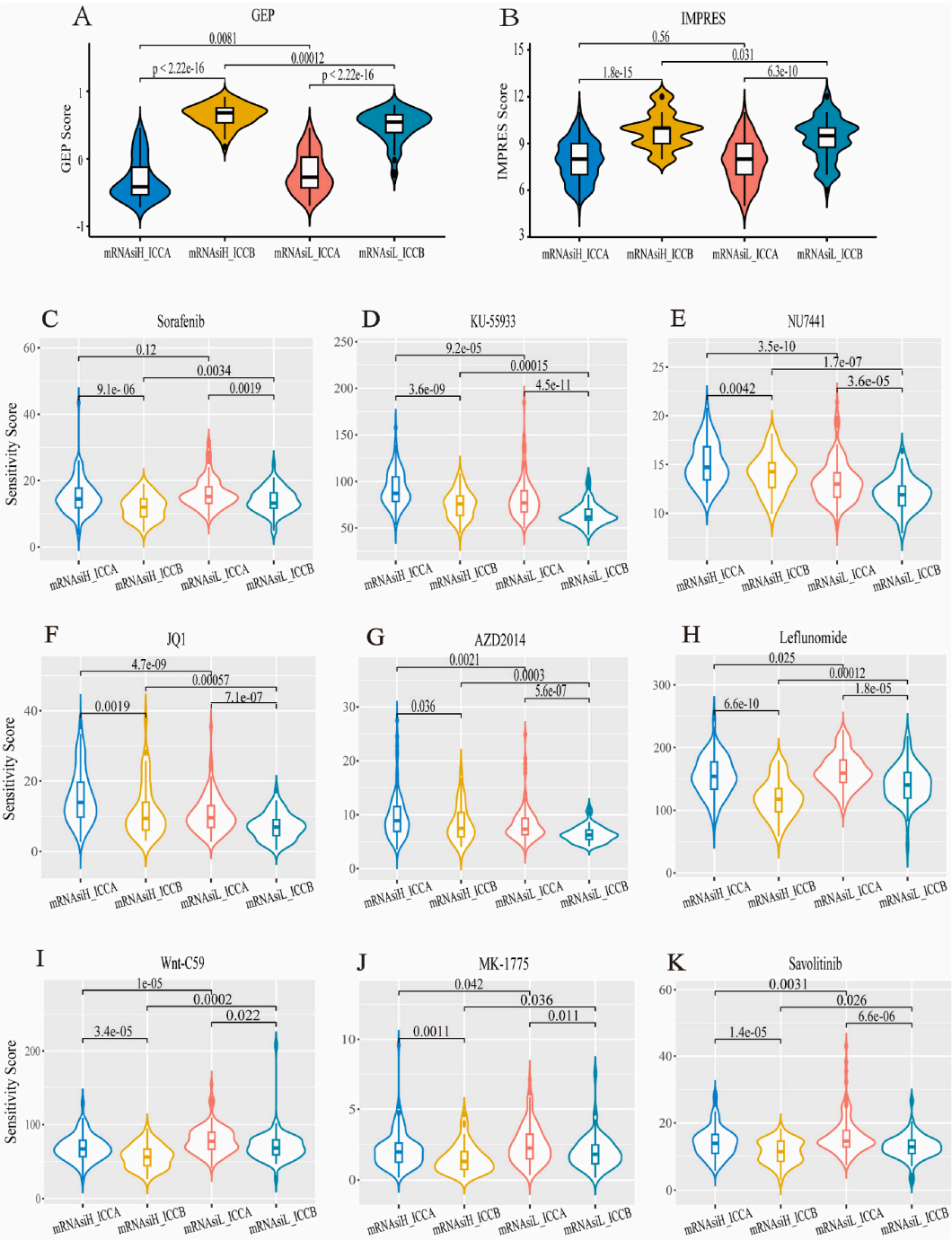

Fig. 6. Immunotherapy response and drug susceptibility estimation of mixed subtypes.(A) GEP Score distribution and comparison of mixed subtypes.(B) IMPRES Score distribution and comparison of mixed subtypes.(C–K) Small molecule drugs IC50 distribution and comparison of mixed subtypes.

3.3. Immunologically related features cluster PLC into two subtypes

Using the k-means consistency clustering method, we evaluated the ability of consensus clustering of immune features on TCGA-LIHC and ICGC-LIRI datasets respectively. The optimal number of clusters was two in both datasets, which can effectively distinguish the sample into two subtypes (Fig. 3A and Fig. S3A). Further survival analysis of the two subtypes showed that there were significant survival differences between the two groups, in which the subset with poor prognosis was named as immune characteristics clustering A (ICC_ A) and the subset with a good prognosis was named immune characteristics clustering B (ICC_B). The OS of ICC_B is significantly longer than that of ICC_ A in TCGA-LIHC (Fig. 3B), and a similar prognosis consequence was observed on the ICGC-LIRI dataset (Fig. S3B).

The composition of TIME was complicated, where various kinds of cells interacted and affected the occurrence, development, and drug resistance of tumors. In order to reveal the immune landscape of immune feature cluster subtypes, we employed the "ESTIMATE" algorithm to quantify the tumor and stromal cells of each sample and found that ICC_B had a higher ImmuneScore, which is accompanied by a higher StromalScore and ESTIMATEScore (Fig. 3C). "CIBERSORT" algorithm depicted the composition of immune cells, and ICC_ B subtype had a high proportion of Macrophages M1, T cells CD4 memory activated, T cells CD8, T cells follicular helper, T cells gamma delta, and T cells regulatory (Tregs). In contrast, Macrophages M2, Mast cells resting, Monocytes and NK cells activated, had a relatively low proportion in ICC_ B subgroup (Fig. 3D). Specifically, analysis of certain immune functional genes within the immune subtype reveals a significant upregulation of immune suppressive genes, immune-activating genes, and human leukocyte antigen genes in ICC_B, indicating the coexistence of immune activation and suppression within this subgroup (Fig. 3E–G). Highly similar immune landscapes were observed in the independent data set ICGC-LIRI (Figs. S3C–G).

3.4. Combined typing construction of prognosis risk score, mRNAsi, and ICC

We implemented three classification strategies in PLC: 12 gene features constructed through data-driven approaches, stem cell subtypes assessed through tumor stem cell similarity evaluation, and immune subtypes clustered based on immune features. We further explored the relationships between subtypes defined by these strategies (Fig. 4A and B). mRNAsi had a significant positive correlation with the risk score of 12 genes constructed by data-driven method ($r = 0.3$, $p = 9.6e\text{-}09$) (Fig. 5A), which further proved that patients in the low mRNAsi subgroup had better survival, indicating that the evaluation of tumor stems cell characteristics was of great significance for patients with liver cancer. The ICC_B subgroup had a lower risk score than the ICC_A subgroup (Fig. 5B) and no significant difference in mRNAsi was observed between ICC subgroups (Fig. 5C). In addition, a large number of patients with high prognostic risk or high mRNAsi had also been observed in the ICC_B subgroup (Fig. 4A–B).

Given the highly positive correlation between the prognostic risk score and the stemness index and the fact that most high-risk patients were in the high mRNAsi subtypes, for comparing conveniently, we mainly paid attention to the subtypes of liver cancer patients differentiated by the combination of stemness index and immune subtypes. We obtained four mixed subtypes by the combined classification, in which those with high mRNAsi in ICC_ A named mRNAsiH_ICCA, those with high mRNAsi in ICC_B named mRNAsiH_ICCB, those with low mRNAsi in ICC_ A named mRNAsiL_ICCA, and those with low mRNAsi in ICC_B named mRNAsiL_ICCB. The combined classification can distinguish subtypes with survival differences. In these mixed subtypes, mRNAsiH_ICCA performed worst and mRNAsiL_ICCB had relatively good survival (Fig. 5D and E).

3.5. Drug efficacy inference of combined subtypes

In order to infer the drug treatment effect of combined subtypes, we evaluated the response of different subtypes to immunotherapy and targeted small-molecule drug therapy. We compared the response markers GEP and IMPRES of immunotherapy efficacy among different subtypes and observed differences in GEP and IMPRES scores, in which the ICC_B group had high scores and the ICC_A was on the opposite. High mRNAsi in ICC_B got the highest scores, indicating that ICC_ B patients were more likely to react to immunotherapy, especially High mRNAsi and ICC_ B might be sensitive to immunotherapy (Fig. 6A and B).

The lower the IC50 value of small-molecular drugs, that is, the lower the sensitivity score, the more sensitive it is to this drug. We found that the IC50 value of each subtype is different among many drugs, in which ICC_B subgroup generally had a lower IC50 value. However, the IC50 performance of different drugs varied between mRNAsi groups within the same immune characteristic subtypes. There was no significant difference for Sorafenib, the first-line drug for liver cancer, between the high and low mRNAsi groups of subgroup ICC_A but the subtype with high mRNAsi had lower IC50 in the ICC_ B, informing that this combination was more sensitive to Sorafenib (Fig. 6C). No matter in ICC_ A or in ICC_B, low mRNAsi subtypes are more sensitive to small molecular drugs that had been reported to have therapeutic or inhibitory effects on liver cancer and liver cancer cell lines, such as KU-55933, NU7441, JQ1, etc. (Fig. 6D–G, Figs. S4C–F). In other drugs such as Leflunomide and Wnt-C59, the high mRNAsi subtype in both two groups had a lower IC50, suggesting a higher sensitivity to small molecular drugs (Fig. 6H–K, Figs. S4G–H).

The results fully corroborated that most ICC_B patients were more sensitive to those drugs, in which ICC_B patients with high mRNAsi were more sensitive subgroups in immunotherapy, Sorafenib, and some drugs. ICC_ A patients, especially with high mRNAsi showed selective drug resistance. The above results suggested that we can distinguish ICC_B which is more sensitive in immunotherapy or small molecular target drugs according to our typing method. In specific drugs, mRNAsi typing can further distinguish more beneficial patient groups.

3.6. Identification of potential compounds for combined subtypes

To determine the drugs that might treat specific subtypes of liver cancer, we screened the significantly up-regulated genes in liver cancer samples as the target of drug inhibition or activation, including the genes that were up-regulated or down-regulated in each subtype and the genes that were specific to a single subtype (Fig. 7A–B). The top 150 genes with the highest upregulation or down-regulation levels were selected and inputted into the query to obtain a score for the drug's ability to reverse gene expression. We sorted the drugs in CMap according to the CMap score and selected several potential compounds according to the score. These drugs had negative scores in liver cancer, that is, had the target gene reversal effect, especially L-16804, ibrutinib were potential therapeutic compounds in all subtypes, and crisotinib in the high ICC_ A subgroup with high mRNAsi had higher potential. CD-437 and KPT-330 in both low mRNAsi and ICC_ A had therapeutic potential and fenretinide in ICC_ B with low mRNAsi had specific therapeutic potential (Fig. 7C).

4. Discussion

In order to better distinguish PLC patients, we integrated three prominent methods of stratification and obtained four subtypes with different prognoses and drug sensitivity. The feasibility of the combined typing strategy was verified by an independent validation dataset. Based on these four subtypes, we predicted the potential targeted drugs of each subtype.

We adopted a variety of machine learnings and Cox regression methods to select prognostic genes and built a 12-gene prognostic risk model, which had good predictive performance in both training and validation sets. Homeobox D9 (HOXD9) regulated and controlled many cells growth, and its overexpression can significantly enhance the migration, invasion and metastasis of hepatocellular carcinoma cells [44]. ALF Transcription Elongation Factor 3 (AFF3) was a susceptibility gene of autoimmune diseases [45]. Compared with normal samples, this gene was low expressed in gastric cancer, but its high expression was associated with poor prognosis of gastric cancer patients [46]. S100 calcium-binding protein A9 (S100A9), a member of the S100 protein family, was a calcium-binding protein that was released as an inflammatory mediator in response to cell damage, infection, or inflammation. Several studies had found that it participated in carcinogenesis and tumor progression, and inhibited tumor immune response [47,48]. Ninjurin 2 (NINJ2) was a novel adhesion molecule and cell experimental evidence showed that the overexpression of NINJ2 promoted the growth of colorectal cancer cells in vitro and in vivo [49]. Paraoxonase 1 (PON1), which was related to high-density lipoprotein (HDL),

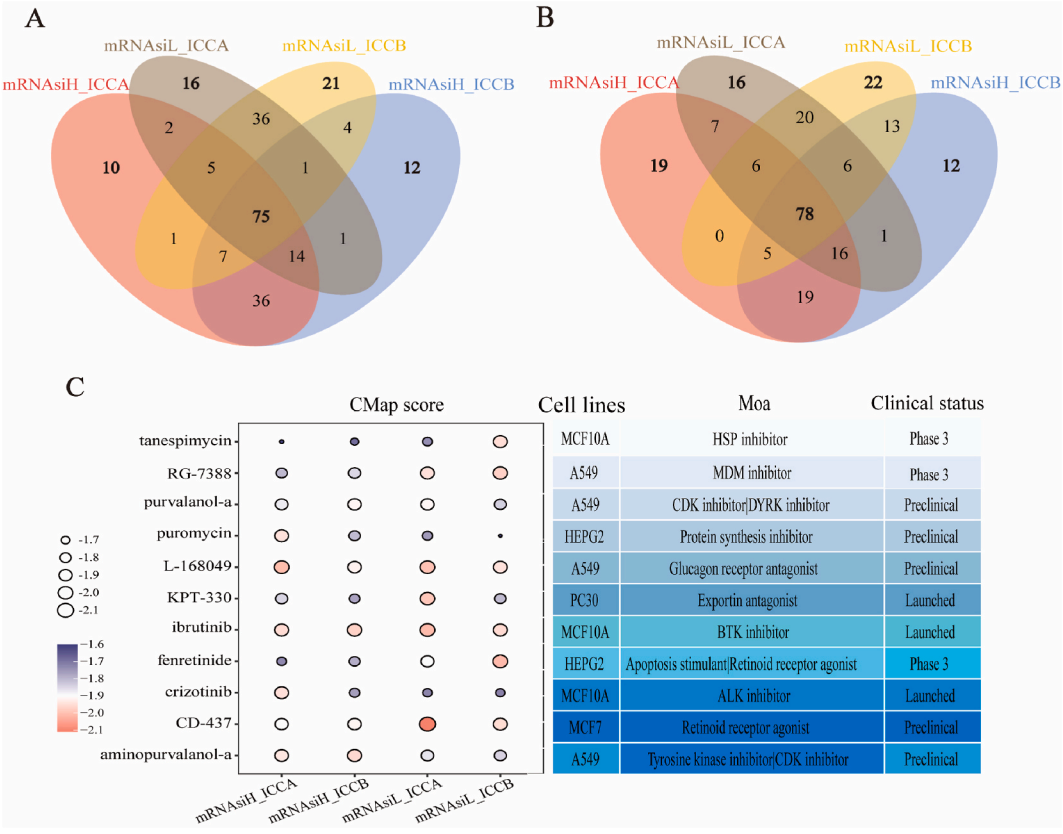

Fig. 7. Potential small molecule drug identification of mixed subtypes. (A) Upregulation of disease genes shared or exclusive in mixed subtypes. (B) Downregulated disease genes shared or exclusive in mixed subtypes. (C) CMap drug prediction for each mixed subtype.

was mainly expressed in the liver and played an antioxidant and anti-inflammatory role [50]. Killer Cell Lectin Like Receptor B1 (KLRB1) encoded cell surface molecule CD161, whose expression can affect tumor immune cell infiltration and the sensitivity of chemotherapy drugs [51]. Suppressor of cycline signaling 2 (SOCS2) regulated the Janus kinase (JAK)/signal transducer and activator of transcription (STAT) pathway negatively, and its importance in various diseases and cancers had been proved [52]. CSC was the root of tumor recurrence and drug resistance. Our study found that in PLC patients with high mRNAsi, many genes necessary for regulating DNA replication, repair and cell cycle process were enriched. E2F_ TARGETS marker gene set was in these enriched gene sets and its corresponding transcription factor regulatory network were the core of cell proliferation control [53]. Many signal molecules can regulate the activity of E2Fs, and E2Fs can transcribe and regulate many different targets, and promote proliferation, self-renewal, transfer and drug resistance, indicating E2F was a potential target for the treatment of PLC [54]. PLC patients with high mRNAsi had a relatively higher TMB, and the loss of p53 function in cancer was related to its effect on CSCs [55,56]. The disorder of P53: Myc axis increased the content and plasticity of CSC, which was the critical factor of tumor growth and clinical invasion [57]. By clustering PLC patients according to immune characteristics in TME, we found that the ICC_B subgroup with better survival had a high proportion of immune cell infiltration. Besides, immune activation and immunosuppression signals coexisted, and some infiltrating immune cells might fail to form immune responses due to immunosuppression [58].

The comprehensive analysis found that the risk score and mRNAsi had a significant positive correlation. Although tumor stem cells and immune system had mutual regulation, patients with high mRNAsi were observed in ICC_B subgroup. mRNAsi and the immune subtypes can capture the tumor stem characteristics and the TME immune characteristics of PLC patients respectively, further refining the stratification of PLC patients through combined typing form, mRNAsiH_ICCA had the worst survival and mRNAsiL_ICCB had the best survival.

At present, one of the important reasons of drug therapy failure for PLC is drug resistance [59]. The patient's immune regulation ability and the strong differentiation potential of CSCs were the crucial factors that led to tumor heterogeneity and further drug response heterogeneity [14,60,61]. Our study found that immunotherapy and other small-molecular drugs had obvious curative effects on ICC_B patients but specific drugs had different therapeutic effects in stemness subgroups. The first-line drug of PLC, sorafenib, was a variety of kinase inhibitors, the number of patients who really benefited significantly from their treatment is very limited [5,62,63], and the cytokine receptor c-Kit(CD117) was one of its targets [64]. It can participate in the regulation of the proliferation and differentiation of hematopoietic stem cells through a series of signal pathways. Blocking the signal transduction of stem cell factor (SCF) - c-Kit can inhibit the proliferation and survival of chemotherapy-induced CSC [65,66]. Therefore, in the ICC_B group, the middle and high stemness subtypes had more significant treatments of sorafenib than the low stemness subtype. Leflunomide was a clinically approved DHODH inhibitor, which can inhibit the proliferation of glioma stem cells, induce DNA damage, and prolong the survival of xenografts of glioblastoma in situ [67]. The therapeutic effect of this drug had been confirmed in hepatocellular carcinoma [68]and this study also observed its specific sensitivity in the high stemness subgroup. KU-55933 was a specific ATM kinase inhibitor and the research found that Sorafenib combined with an ATM inhibitor had a synergistic anti-tumor effect in the treatment of hepatocellular carcinoma cells [69]. The results of this study showed that inhibiting the proliferation or functional products of CSCs was a possible way to reverse drug resistance. The hinge to successful cancer treatment was targeting CSCs [70], suggesting the importance of combined targeted therapy. In addition, this study also found that a selective estrogen receptor degradation agent (GDC0810) [71] and a selective LRRK2 kinase inhibitor (GSK2578215A) [72] were sensitive in the PLC subgroup with obvious stemness characteristics. No research report had shown their inhibitory effect on hepatoma cells or tumor stem cells, and whether they target hepatoma stem cells needed further study.

In order to explore the treatment strategies corresponding to different subtypes and increase clinical availability, we employed CMap analysis to unearth potential targeted gene compounds of each subtype, thus laying a foundation for treatment research. Crisotinib in ICC_ A group with high mRNAsi, the worst survival subgroup, had been observed a specific ability to reverse disease genes. The recent reports demonstrated that ALK inhibitors in soft tissue sarcomas can inhibit the carcinogenic function of ALKATI, and also weaken the CSC-like characteristics of ALKATI induced by reducing the expression of stem cell markers in vitro and in vivo [73], showing crisotinib was a potential therapeutic drug for patients with high stemness characteristics. CD-437 was a kind of retinol-like molecule, which had been observed to induce apoptosis of hepatoma cells through mitochondrial pathway [74,75]. CD-437's ability to reverse disease gene expression was observed in four subtypes, especially the mRNAsiL_ICCB subtype. In future work, it is necessary to further evaluate the potential of identified drugs in treating PLC.

5. Conclusions

In conclusion, tumor heterogeneity affects the occurrence, development, and treatment response of cancers, ultimately leading to differences in patient prognosis. By combined typing strategy, we identified PLC subtypes with different biological characteristics, drug sensitivity, and prognosis, providing a feasible hierarchical standard for the precise treatment of PLC. Further analysis, based on specific gene expression characteristics, predicted potential therapeutic drugs that regulated the expression of disease signature genes in each subtype. We hope our study can be valuable for clinical therapy, providing new insight for the research of liver cancer.

Data availability statement

Data included in article/supp. Material/referenced in article. This study used the following publicly available datasets: TCGA-LIHC in TCGA (https://xenabrowser.net/), ICGC-LIRI in ICGC (https://dcc.icgc.org/).

Funding statement

This research was funded by (National Natural Science Foundation of China), grant number (82204159) and by (Postdoctoral Fund project of Chongqing), grant number (cstc2021jcyj-bshX0220).

CRediT authorship contribution statement

Jielian Deng: Writing – original draft, Methodology, Investigation, Formal analysis, Conceptualization. **Guichuan Lai:** Software. **Cong Zhang:** Writing – original draft, Visualization. **Kangjie Li:** Validation, Data curation. **WenYan Zhu:** Supervision, Conceptualization. **Biao Xie:** Writing – review & editing, Supervision, Methodology, Funding acquisition. **Xiaoni Zhong:** Writing – review & editing, Supervision, Investigation, Funding acquisition, Conceptualization.

Declaration of competing interest

The authors declare that they have no known competing financial interests or personal relationships that could have appeared to influence the work reported in this paper.

Acknowledgments

We are very appreciated TCGA, ICGC and PCBC databases for providing relevant data to support our studies.

Appendix A. Supplementary data

Supplementary data to this article can be found online at https://doi.org/10.1016/j.heliyon.2024.e25570.

References

[1] K.A. McGlynn, J.L. Petrick, H.B. El-Serag, Epidemiology of hepatocellular carcinoma, Hepatology 73 (2021) 4–13, https://doi.org/10.1002/hep.31288.
[2] H. Rumgay, M. Arnold, J. Ferlay, O. Lesi, C.J. Cabasag, J. Vignat, M. Laversanne, K.A. McGlynn, I. Soerjomataram, Global burden of primary liver cancer in 2020 and predictions to 2040, J. Hepatol. 77 (2022) 1598–1606, https://doi.org/10.1016/j.jhep.2022.08.021.
[3] H. Sung, J. Ferlay, R.L. Siegel, M. Laversanne, I. Soerjomataram, A. Jemal, F. Bray, Global cancer statistics 2020: GLOBOCAN estimates of incidence and mortality worldwide for 36 cancers in 185 countries, CA A Cancer J. Clin. 71 (2021) 209–249, https://doi.org/10.3322/caac.21660.
[4] A. Forner, M. Reig, J. Bruix, Hepatocellular carcinoma, Lancet 391 (2018) 1301–1314, https://doi.org/10.1016/S0140-6736(18)30010-2.
[5] J.M. Llovet, R. Montal, D. Sia, R.S. Finn, Molecular therapies and precision medicine for hepatocellular carcinoma, Nat. Rev. Clin. Oncol. 15 (2018) 599–616, https://doi.org/10.1038/s41571-018-0073-4.
[6] Y. Zheng, S. Wang, J. Cai, A. Ke, J. Fan, The progress of immune checkpoint therapy in primary liver cancer, Biochim. Biophys. Acta Rev. Canc 1876 (2021) 188638, https://doi.org/10.1016/j.bbcan.2021.188638.
[7] J. Liu, H. Dang, X.W. Wang, The significance of intertumor and intratumor heterogeneity in liver cancer, Exp. Mol. Med. 50 (2018), https://doi.org/10.1038/emm.2017.165 e416–e416.
[8] D.R. Welch, Tumor heterogeneity—a 'contemporary concept' founded on historical insights and predictions, Cancer Res. 76 (2016) 4–6, https://doi.org/10.1158/0008-5472.CAN-15-3024.
[9] I. Dagogo-Jack, A.T. Shaw, Tumour heterogeneity and resistance to cancer therapies, Nat. Rev. Clin. Oncol. 15 (2018) 81–94, https://doi.org/10.1038/nrclinonc.2017.166.
[10] N.M. Anderson, M.C. Simon, The tumor microenvironment, Curr. Biol. 30 (2020) R921–R925, https://doi.org/10.1016/j.cub.2020.06.081.
[11] L.-K. Chan, Y.-M. Tsui, D.W.-H. Ho, I.O.-L. Ng, Cellular heterogeneity and plasticity in liver cancer, Semin. Cancer Biol. 82 (2022) 134–149, https://doi.org/10.1016/j.semcancer.2021.02.015.
[12] C.J. Pelham, M. Nagane, E. Madan, Cell competition in tumor evolution and heterogeneity: merging past and present, Semin. Cancer Biol. 63 (2020) 11–18, https://doi.org/10.1016/j.semcancer.2019.07.008.
[13] P.R. Prasetyanti, J.P. Medema, Intra-tumor heterogeneity from a cancer stem cell perspective, Mol. Cancer 16 (2017) 41, https://doi.org/10.1186/s12943-017-0600-4.
[14] A. Carnero, Y. Garcia-Mayea, C. Mir, J. Lorente, I.T. Rubio, M.E. Lleonart, The cancer stem-cell signaling network and resistance to therapy, Cancer Treat Rev. 49 (2016) 25–36, https://doi.org/10.1016/j.ctrv.2016.07.001.
[15] X. Ren, L. Zhang, Y. Zhang, Z. Li, N. Siemers, Z. Zhang, Insights gained from single-cell analysis of immune cells in the tumor microenvironment, Annu. Rev. Immunol. 39 (2021) 583–609, https://doi.org/10.1146/annurev-immunol-110519-071134.
[16] Q. Duan, H. Zhang, J. Zheng, L. Zhang, Turning cold into hot: firing up the tumor microenvironment, Trends in Cancer 6 (2020) 605–618, https://doi.org/10.1016/j.trecan.2020.02.022.
[17] P.H.D. Nguyen, S. Ma, C.Z.J. Phua, N.A. Kaya, H.L.H. Lai, C.J. Lim, J.Q. Lim, M. Wasser, L. Lai, W.L. Tam, T.K.H. Lim, W.K. Wan, T. Loh, W.Q. Leow, Y.H. Pang, C.Y. Chan, S.Y. Lee, P.C. Cheow, H.C. Toh, F. Ginhoux, S. Iyer, A.W.C. Kow, Y. Young Dan, A. Chung, G.K. Bonney, B.K.P. Goh, S. Albani, P.K.H. Chow, W. Zhai, V. Chew, Intratumoural immune heterogeneity as a hallmark of tumour evolution and progression in hepatocellular carcinoma, Nat. Commun. 12 (2021) 227, https://doi.org/10.1038/s41467-020-20171-7.
[18] Y. Tang, L. Xu, Y. Ren, Y. Li, F. Yuan, M. Cao, Y. Zhang, M. Deng, Z. Yao, Identification and validation of a prognostic model based on three MVI-related genes in hepatocellular carcinoma, Int. J. Biol. Sci. 18 (2022) 261–275, https://doi.org/10.7150/ijbs.66536.
[19] M. Zhao, S. Shen, C. Xue, A novel m1A-score model correlated with the immune microenvironment predicts prognosis in hepatocellular carcinoma, Front. Immunol. 13 (2022) 805967, https://doi.org/10.3389/fimmu.2022.805967.
[20] C. Wang, S. Qin, W. Pan, X. Shi, H. Gao, P. Jin, X. Xia, F. Ma, mRNAsi-related genes can effectively distinguish hepatocellular carcinoma into new molecular subtypes, Comput. Struct. Biotechnol. J. 20 (2022) 2928–2941, https://doi.org/10.1016/j.csbj.2022.06.011.
[21] B. Hu, X.-B. Yang, X.-T. Sang, Molecular subtypes based on immune-related genes predict the prognosis for hepatocellular carcinoma patients, Int. Immunopharm. 90 (2021) 107164, https://doi.org/10.1016/j.intimp.2020.107164.

[22] D. Bayik, J.D. Lathia, Cancer stem cell–immune cell crosstalk in tumour progression, Nat. Rev. Cancer 21 (2021) 526–536, https://doi.org/10.1038/s41568-021-00366-w.

[23] B.T. Lee, G.P. Barber, A. Benet-Pagès, J. Casper, H. Clawson, M. Diekhans, C. Fischer, J.N. Gonzalez, A.S. Hinrichs, C.M. Lee, P. Muthuraman, L.R. Nassar, B. Nguy, T. Pereira, G. Perez, B.J. Raney, K.R. Rosenbloom, D. Schmelter, M.L. Speir, B.D. Wick, A.S. Zweig, D. Haussler, R.M. Kuhn, M. Haeussler, W.J. Kent, The UCSC Genome Browser database: 2022 update, Nucleic Acids Res. 50 (2022) D1115–D1122, https://doi.org/10.1093/nar/gkab959.

[24] F. Wu, G.-Z. Li, H.-J. Liu, Z. Zhao, R.-C. Chai, Y.-Q. Liu, H.-Y. Jiang, Y. Zhai, Y.-M. Feng, R.-P. Li, W. Zhang, Molecular subtyping reveals immune alterations in IDH wild-type lower-grade diffuse glioma, J. Pathol. 251 (2020) 272–283, https://doi.org/10.1002/path.5468.

[25] H.K. Joon, A. Thalor, D. Gupta, Machine learning analysis of lung squamous cell carcinoma gene expression datasets reveals novel prognostic signatures, Comput. Biol. Med. 165 (2023) 107430, https://doi.org/10.1016/j.compbiomed.2023.107430.

[26] Z. Zheng, W. Xie, X. Chen, F. Wang, L. Huang, X. Li, Q. Lin, K.-C. Wong, Subclass-specific prognosis and treatment efficacy inference in head and neck squamous carcinoma, IEEE J Biomed Health Inform 26 (2022) 4303–4313, https://doi.org/10.1109/JBHI.2022.3168289.

[27] T.M. Malta, A. Sokolov, A.J. Gentles, T. Burzykowski, L. Poisson, J.N. Weinstein, B. Kamińska, J. Huelsken, L. Omberg, O. Gevaert, A. Colaprico, P. Czerwińska, S. Mazurek, L. Mishra, H. Heyn, A. Krasnitz, A.K. Godwin, A.J. Lazar, Cancer Genome Atlas Research Network, J.M. Stuart, K.A. Hoadley, P.W. Laird, H. Noushmehr, M. Wiznerowicz, Machine learning identifies stemness features associated with oncogenic dedifferentiation, Cell 173 (2018) 338–354, https://doi.org/10.1016/j.cell.2018.03.034, e15.

[28] H. Lian, Y.-P. Han, Y.-C. Zhang, Y. Zhao, S. Yan, Q.-F. Li, B.-C. Wang, J.-J. Wang, W. Meng, J. Yang, Q.-H. Wang, W.-W. Mao, J. Ma, Integrative analysis of gene expression and DNA methylation through one-class logistic regression machine learning identifies stemness features in medulloblastoma, Mol. Oncol. 13 (2019) 2227–2245, https://doi.org/10.1002/1878-0261.12557.

[29] P. Charoentong, F. Finotello, M. Angelova, C. Mayer, M. Efremova, D. Rieder, H. Hackl, Z. Trajanoski, Pan-cancer immunogenomic analyses reveal genotype-immunophenotype relationships and predictors of response to checkpoint blockade, Cell Rep. 18 (2017) 248–262, https://doi.org/10.1016/j.celrep.2016.12.019.

[30] S. Hänzelmann, R. Castelo, J. Guinney, GSVA: gene set variation analysis for microarray and RNA-Seq data, BMC Bioinf. 14 (2013) 7, https://doi.org/10.1186/1471-2105-14-7.

[31] M.D. Wilkerson, D.N. Hayes, ConsensusClusterPlus: a class discovery tool with confidence assessments and item tracking, Bioinformatics 26 (2010) 1572–1573, https://doi.org/10.1093/bioinformatics/btq170.

[32] A.M. Newman, C.L. Liu, M.R. Green, A.J. Gentles, W. Feng, Y. Xu, C.D. Hoang, M. Diehn, A.A. Alizadeh, Robust enumeration of cell subsets from tissue expression profiles, Nat. Methods 12 (2015) 453–457, https://doi.org/10.1038/nmeth.3337.

[33] K. Yoshihara, M. Shahmoradgoli, E. Martínez, R. Vegesna, H. Kim, W. Torres-Garcia, V. Treviño, H. Shen, P.W. Laird, D.A. Levine, S.L. Carter, G. Getz, K. Stemke-Hale, G.B. Mills, R.G.W. Verhaak, Inferring tumour purity and stromal and immune cell admixture from expression data, Nat. Commun. 4 (2013) 2612, https://doi.org/10.1038/ncomms3612.

[34] T. Wu, E. Hu, S. Xu, M. Chen, P. Guo, Z. Dai, T. Feng, L. Zhou, W. Tang, L. Zhan, X. Fu, S. Liu, X. Bo, G. Yu, clusterProfiler 4.0: a universal enrichment tool for interpreting omics data, Innovation 2 (2021) 100141, https://doi.org/10.1016/j.xinn.2021.100141.

[35] M.E. Ritchie, B. Phipson, D. Wu, Y. Hu, C.W. Law, W. Shi, G.K. Smyth, Limma powers differential expression analyses for RNA-sequencing and microarray studies, Nucleic Acids Res. 43 (2015), https://doi.org/10.1093/nar/gkv007 e47–e47.

[36] A. Mayakonda, D.-C. Lin, Y. Assenov, C. Plass, H.P. Koeffler, Maftools: efficient and comprehensive analysis of somatic variants in cancer, Genome Res. 28 (2018) 1747–1756, https://doi.org/10.1101/gr.239244.118.

[37] M. Ayers, J. Lunceford, M. Nebozhyn, E. Murphy, A. Loboda, D.R. Kaufman, A. Albright, J.D. Cheng, S.P. Kang, V. Shankaran, S.A. Piha-Paul, J. Yearley, T. Y. Seiwert, A. Ribas, T.K. McClanahan, IFN-γ–related mRNA profile predicts clinical response to PD-1 blockade, J. Clin. Invest. 127 (2017) 2930–2940, https://doi.org/10.1172/JCI91190.

[38] R. Cristescu, R. Mogg, M. Ayers, A. Albright, E. Murphy, J. Yearley, X. Sher, X.Q. Liu, H. Lu, M. Nebozhyn, C. Zhang, J.K. Lunceford, A. Joe, J. Cheng, A. L. Webber, N. Ibrahim, E.R. Plimack, P.A. Ott, T.Y. Seiwert, A. Ribas, T.K. McClanahan, J.E. Tomassini, A. Loboda, D. Kaufman, Pan-tumor genomic biomarkers for PD-1 checkpoint blockade–based immunotherapy, Science 362 (2018), https://doi.org/10.1126/science.aar3593 eaar3593.

[39] N. Auslander, G. Zhang, J.S. Lee, D.T. Frederick, B. Miao, T. Moll, T. Tian, Z. Wei, S. Madan, R.J. Sullivan, G. Boland, K. Flaherty, M. Herlyn, E. Ruppin, Robust prediction of response to immune checkpoint blockade therapy in metastatic melanoma, Nat. Med. 24 (2018) 1545–1549, https://doi.org/10.1038/s41591-018-0157-9.

[40] R. Chen, X. Wang, X. Deng, L. Chen, Z. Liu, D. Li, CPDR: an R package of recommending personalized drugs for cancer patients by reversing the individual's disease-related signature, Front. Pharmacol. 13 (2022) 904909, https://doi.org/10.3389/fphar.2022.904909.

[41] J. Lamb, The Connectivity Map: a new tool for biomedical research, Nat. Rev. Cancer 7 (2007) 54–60, https://doi.org/10.1038/nrc2044.

[42] J. Liang, D. Wang, H. Lin, X. Chen, H. Yang, Y. Zheng, Y. Li, A novel ferroptosis-related gene signature for overall survival prediction in patients with hepatocellular carcinoma, Int. J. Biol. Sci. 16 (2020) 2430–2441, https://doi.org/10.7150/ijbs.45050.

[43] Q. He, J. Yang, Y. Jin, Immune infiltration and clinical significance analyses of the coagulation-related genes in hepatocellular carcinoma, Briefings Bioinf. 23 (2022), https://doi.org/10.1093/bib/bbac291 bbac291.

[44] X. Lv, L. Li, L. Lv, X. Qu, S. Jin, K. Li, X. Deng, L. Cheng, H. He, L. Dong, HOXD9 promotes epithelial–mesenchymal transition and cancer metastasis by ZEB1 regulation in hepatocellular carcinoma, J. Exp. Clin. Cancer Res. 34 (2015) 133, https://doi.org/10.1186/s13046-015-0245-3.

[45] S. Tsukumo, P.G. Subramani, N. Seija, M. Tabata, Y. Maekawa, Y. Mori, C. Ishifune, Y. Itoh, M. Ota, K. Fujio, J.M. Di Noia, K. Yasutomo, AFF3, a susceptibility factor for autoimmune diseases, is a molecular facilitator of immunoglobulin class switch recombination, Sci. Adv. 8 (2022) eabq0008, https://doi.org/10.1126/sciadv.abq0008.

[46] Y. Zeng, X. Zhang, F. Li, Y. Wang, M. Wei, AFF3 Is a Novel Prognostic Biomarker and a Potential Target for Immunotherapy in Gastric Cancer, vol. 36, Clinical Laboratory Analysis, 2022, https://doi.org/10.1002/jcla.24437.

[47] C. Zhong, Y. Niu, W. Liu, Y. Yuan, K. Li, Y. Shi, Z. Qiu, K. Li, Z. Lin, Z. Huang, D. Zuo, Z. Yang, Y. Liao, Y. Zhang, C. Wang, J. Qiu, W. He, Y. Yuan, B. Li, S100A9 derived from chemoembolization-induced hypoxia governs mitochondrial function in hepatocellular carcinoma progression, Adv. Sci. 9 (2022) e2202206, https://doi.org/10.1002/advs.202202206.

[48] M. Huang, R. Wu, L. Chen, Q. Peng, S. Li, Y. Zhang, L. Zhou, L. Duan, S100A9 regulates MDSCs-mediated immune suppression via the RAGE and TLR4 signaling pathways in colorectal carcinoma, Front. Immunol. 10 (2019) 2243, https://doi.org/10.3389/fimmu.2019.02243.

[49] G. Li, L.-N. Zhou, H. Yang, X. He, Y. Duan, F. Wu, Ninjurin 2 overexpression promotes human colorectal cancer cell growth in vitro and in vivo, Aging 11 (2019) 8526–8541, https://doi.org/10.18632/aging.102336.

[50] T. Bacchetti, G. Ferretti, A. Sahebkar, The role of paraoxonase in cancer, Semin. Cancer Biol. 56 (2019) 72–86, https://doi.org/10.1016/j.semcancer.2017.11.013.

[51] C.L. Duurland, S.J. Santegoets, Z. Abdulrahman, N.M. Loof, G. Sturm, T.H. Wesselink, R. Arens, S. Boekestijn, I. Ehsan, M.I.E. van Poelgeest, F. Finotello, H. Hackl, Z. Trajanoski, P. ten Dijke, V.M. Braud, M.J.P. Welters, S.H. van der Burg, CD161 expression and regulation defines rapidly responding effector CD4+ T cells associated with improved survival in HPV16-associated tumors, J Immunother Cancer 10 (2022) e003995, https://doi.org/10.1136/jitc-2021-003995.

[52] W. Ren, S. Wu, Y. Wu, T. Liu, X. Zhao, Y. Li, MicroRNA-196a/-196b regulate the progression of hepatocellular carcinoma through modulating the JAK/STAT pathway via targeting SOCS2, Cell Death Dis. 10 (2019) 333, https://doi.org/10.1038/s41419-019-1530-4.

[53] L.N. Kent, G. Leone, The broken cycle: E2F dysfunction in cancer, Nat. Rev. Cancer 19 (2019) 326–338, https://doi.org/10.1038/s41568-019-0143-7.

[54] D. Xie, Q. Pei, J. Li, X. Wan, T. Ye, Emerging role of E2F family in cancer stem cells, Front. Oncol. 11 (2021) 723137, https://doi.org/10.3389/fonc.2021.723137.

[55] G. Koifman, Y. Shetzer, S. Eizenberger, H. Solomon, R. Rotkopf, A. Molchadsky, G. Lonetto, N. Goldfinger, V. Rotter, A mutant p53-dependent embryonic stem cell gene signature is associated with augmented tumorigenesis of stem cells, Cancer Res. 78 (2018) 5833–5847, https://doi.org/10.1158/0008-5472.CAN-18-0805.

[56] H. Zheng, H. Ying, H. Yan, A.C. Kimmelman, D.J. Hiller, A.-J. Chen, S.R. Perry, G. Tonon, G.C. Chu, Z. Ding, J.M. Stommel, K.L. Dunn, R. Wiedemeyer, M.J. You, C. Brennan, Y.A. Wang, K.L. Ligon, W.H. Wong, L. Chin, R.A. DePinho, p53 and Pten control neural and glioma stem/progenitor cell renewal and differentiation, Nature 455 (2008) 1129–1133, https://doi.org/10.1038/nature07443.
[57] A. Santoro, T. Vlachou, L. Luzi, G. Melloni, L. Mazzarella, E. D'Elia, X. Aobuli, C.E. Pasi, L. Reavie, P. Bonetti, S. Punzi, L. Casoli, A. Sabò, M.C. Moroni, G. I. Dellino, B. Amati, F. Nicassio, L. Lanfrancone, P.G. Pelicci, p53 loss in breast cancer leads to Myc activation, increased cell plasticity, and expression of a mitotic signature with prognostic value, Cell Rep. 26 (2019) 624–638.e8, https://doi.org/10.1016/j.celrep.2018.12.071.
[58] O.V. Makarova-Rusher, J. Medina-Echeverz, A.G. Duffy, T.F. Greten, The yin and yang of evasion and immune activation in HCC, J. Hepatol. 62 (2015) 1420–1429, https://doi.org/10.1016/j.jhep.2015.02.038.
[59] T.F. Greten, C.W. Lai, G. Li, K.F. Staveley-O'Carroll, Targeted and immune-based therapies for hepatocellular carcinoma, Gastroenterology 156 (2019) 510–524, https://doi.org/10.1053/j.gastro.2018.09.051.
[60] C. Box, S.J. Rogers, M. Mendiola, S.A. Eccles, Tumour-microenvironmental interactions: paths to progression and targets for treatment, Semin. Cancer Biol. 20 (2010) 128–138, https://doi.org/10.1016/j.semcancer.2010.06.004.
[61] K. Thol, P. Pawlik, N. McGranahan, Therapy sculpts the complex interplay between cancer and the immune system during tumour evolution, Genome Med. 14 (2022) 137, https://doi.org/10.1186/s13073-022-01138-3.
[62] Z. Cheng, J. Wei-Qi, D. Jin, New insights on sorafenib resistance in liver cancer with correlation of individualized therapy, Biochim. Biophys. Acta Rev. Canc 1874 (2020) 188382, https://doi.org/10.1016/j.bbcan.2020.188382.
[63] W. Tang, Z. Chen, W. Zhang, Y. Cheng, B. Zhang, F. Wu, Q. Wang, S. Wang, D. Rong, F.P. Reiter, E.N. De Toni, X. Wang, The mechanisms of sorafenib resistance in hepatocellular carcinoma: theoretical basis and therapeutic aspects, Signal Transduct. Targeted Ther. 5 (2020) 87, https://doi.org/10.1038/s41392-020-0187-x.
[64] S. Bracarda, C. Caserta, L. Sordini, M. Rossi, A. Hamzay, L. Crinò, Protein kinase inhibitors in the treatment of renal cell carcinoma: sorafenib, Ann. Oncol. 18 (2007) vi22–vi25, https://doi.org/10.1093/annonc/mdm219.
[65] E.L. Mazzoldi, S. Pavan, G. Pilotto, K. Leone, A. Pagotto, S. Frezzini, M.O. Nicoletto, A. Amadori, A. Pastò, A juxtacrine/paracrine loop between C-Kit and stem cell factor promotes cancer stem cell survival in epithelial ovarian cancer, Cell Death Dis. 10 (2019) 412, https://doi.org/10.1038/s41419-019-1656-4.
[66] V. Levina, A. Marrangoni, T. Wang, S. Parikh, Y. Su, R. Herberman, A. Lokshin, E. Gorelik, Elimination of human lung cancer stem cells through targeting of the stem cell factor–c-kit autocrine signaling loop, Cancer Res. 70 (2010) 338–346, https://doi.org/10.1158/0008-5472.CAN-09-1102.
[67] R. Spina, I. Mills, F. Ahmad, C. Chen, H.M. Ames, J.A. Winkles, G.F. Woodworth, E.E. Bar, DHODH inhibition impedes glioma stem cell proliferation, induces DNA damage, and prolongs survival in orthotopic glioblastoma xenografts, Oncogene 41 (2022) 5361–5372, https://doi.org/10.1038/s41388-022-02517-1.
[68] Z. Zhu, C. Cao, D. Zhang, Z. Zhang, L. Liu, D. Wu, J. Sun, UBE2T-mediated Akt ubiquitination and Akt/β-catenin activation promotes hepatocellular carcinoma development by increasing pyrimidine metabolism, Cell Death Dis. 13 (2022) 154, https://doi.org/10.1038/s41419-022-04596-0.
[69] J. Liu, Y. Liu, L. Meng, B. Ji, D. Yang, Synergistic antitumor effect of sorafenib in combination with ATM inhibitor in hepatocellular carcinoma cells, Int. J. Med. Sci. 14 (2017) 523–529, https://doi.org/10.7150/ijms.19033.
[70] J.A. Clara, C. Monge, Y. Yang, N. Takebe, Targeting signalling pathways and the immune microenvironment of cancer stem cells — a clinical update, Nat. Rev. Clin. Oncol. 17 (2020) 204–232, https://doi.org/10.1038/s41571-019-0293-2.
[71] A. Lai, M. Kahraman, S. Govek, J. Nagasawa, C. Bonnefous, J. Julien, K. Douglas, J. Sensintaffar, N. Lu, K. Lee, A. Aparicio, J. Kaufman, J. Qian, G. Shao, R. Prudente, M.J. Moon, J.D. Joseph, B. Darimont, D. Brigham, K. Grillot, R. Heyman, P.J. Rix, J.H. Hager, N.D. Smith, Identification of GDC-0810 (ARN-810), an orally bioavailable selective estrogen receptor degrader (SERD) that demonstrates robust activity in tamoxifen-resistant breast cancer xenografts, J. Med. Chem. 58 (2015) 4888–4904, https://doi.org/10.1021/acs.jmedchem.5b00054.
[72] S. Saez-Atienzar, L. Bonet-Ponce, J.R. Blesa, F.J. Romero, M.P. Murphy, J. Jordan, M.F. Galindo, The LRRK2 inhibitor GSK2578215A induces protective autophagy in SH-SY5Y cells: involvement of Drp-1-mediated mitochondrial fission and mitochondrial-derived ROS signaling, Cell Death Dis. 5 (2014), https://doi.org/10.1038/cddis.2014.320 e1368–e1368.
[73] B.-S. Xu, H.-Y. Chen, Y. Que, W. Xiao, M.-S. Zeng, X. Zhang, ALKATI interacts with c-Myc and promotes cancer stem cell-like properties in sarcoma, Oncogene 39 (2020) 151–163, https://doi.org/10.1038/s41388-019-0973-5.
[74] K. Gonda, H. Tsuchiya, T. Sakabe, Y. Akechi, R. Ikeda, R. Nishio, K. Terabayashi, K. Ishii, Y. Matsumi, A.A. Ashla, H. Okamoto, K. Takubo, S. Matsuoka, Y. Watanabe, Y. Hoshikawa, A. Kurimasa, G. Shiota, Synthetic retinoid CD437 induces mitochondria-mediated apoptosis in hepatocellular carcinoma cells, Biochem. Biophys. Res. Commun. 370 (2008) 629–633, https://doi.org/10.1016/j.bbrc.2008.04.008.
[75] T. Han, M. Goralski, E. Capota, S.B. Padrick, J. Kim, Y. Xie, D. Nijhawan, The antitumor toxin CD437 is a direct inhibitor of DNA polymerase α, Nat. Chem. Biol. 12 (2016) 511–515, https://doi.org/10.1038/nchembio.2082.